

First Principles Calculations of Hydrogen Evolution Reaction and Proton Migration on Stepped Surfaces of SrTiO₃

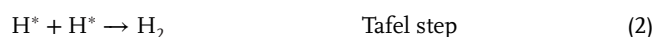
Maksim Sokolov,* Yuri A. Mastrikov, Guntars Zvejnieks, Dmitry Bocharov, Veera Krasnenko, Kai S. Exner, and Eugene A. Kotomin

Recent research suggests that photocatalytic activity toward water splitting of strontium titanate SrTiO₃ (STO) is enhanced by creating multifaceted nanoparticles. To better understand the source of this activity, a previously designed model is used for two types of surfaces of this nanoparticle, flat and double-stepped. Density functional theory calculations of water adsorption on these surfaces are performed to gain insight into water adsorption and proton migration processes, as well as thermodynamics of hydrogen evolution reaction within the framework of computational hydrogen electrode. It is concluded that ridges of single- and double-stepped surfaces are nearly identical in terms of adsorption configurations and energetics. Also, it is demonstrated that protons have migration barriers lower than 0.7 eV and that surface morphology impacts catalytic activity toward hydrogen evolution reaction, with flat surface demonstrating higher catalytic activity.

1. Introduction

There is a great interest in developing intermittent renewable energy sources, such as wind turbines or solar panels. One possible improvement direction is toward storage of overproduced energy by using hydrogen as energy vector. Hydrogen itself is produced in hydrogen evolution reaction (HER), which is cathodic half-reaction of electro- or photocatalytic water splitting. HER reaction equation is $2\text{H}^+ + 2\text{e}^- \rightarrow \text{H}_2(\text{g})$, $U^0 = 0$ V versus reversible hydrogen electrode (RHE). There are two different mechanisms of HER: Volmer–Tafel (V–T) mechanism and Volmer–Heyrovsky (V–H) mechanism. The V–T mechanism consists of two Volmer steps, which are

adsorption of two hydrogen atoms to the active site, denoted as * (Equation (1)), followed by recombination of two adjacent hydrogen atoms and desorption, or Tafel step (Equation (2)) to form gaseous H₂. V–H mechanism, however, comprises of a single Volmer step, and the second hydrogen atom is taken from the surrounding media (Heyrovsky step, Equation (3)).



Strontium titanate SrTiO₃ (STO) is a good catalyst for overall water splitting and HER in particular.^[1–14] The catalytic activity of STO toward water splitting can be further improved by creating faceted nanoparticles.^[15] Such an improvement is attributed to preferential deposition of Pt and Co₃O₄ co-catalyst, as well as lower charge recombination rate. Both of these factors arise due to anisotropy of the multifaceted nanoparticles.

Water adsorption on STO was studied in detail.^[16–18] In the previous paper our group investigated adsorption configuration and energetics of water on two types of surfaces of faceted nanoparticles, namely, flat {001} and stepped {110}.^[19] However, HER on STO stepped surface has not yet been described.

In this paper we continue our research by investigating water dissociation and proton migration to deeper understand process of HER on STO stepped surface. We estimate transition energy barriers for the proton migration and demonstrate that V–T

M. Sokolov, Y. A. Mastrikov, G. Zvejnieks, D. Bocharov, E. A. Kotomin
Institute of Solid State Physics
University of Latvia
Kengaraga 8, Riga LV1063, Latvia
E-mail: maksim.sokolov@uni-due.de


M. Sokolov, K. S. Exner
Theoretical Inorganic Chemistry
University of Duisburg-Essen
Universitätsstraße 5, 545141 Essen, Germany

V. Krasnenko
Institute of Physics
University of Tartu
W. Ostwaldi Str 1, Tartu 50411, Estonia

K. S. Exner
Cluster of Excellence RESOLV
Ruhr-University Bochum
Universitätsstraße 150, 47057 Bochum, Germany

K. S. Exner
Center for Nanointegration (CENIDE) Duisburg-Essen
University of Duisburg-Essen
Carl-Benz-Straße 199, 47057 Duisburg, Germany

E. A. Kotomin
Physical Chemistry of Solids
Max Planck Institute for Solid State Research
Heisenbergstraße 1, 70569 Stuttgart, Germany

 The ORCID identification number(s) for the author(s) of this article can be found under <https://doi.org/10.1002/adts.202200619>

© 2023 The Authors. Advanced Theory and Simulations published by Wiley-VCH GmbH. This is an open access article under the terms of the Creative Commons Attribution-NonCommercial License, which permits use, distribution and reproduction in any medium, provided the original work is properly cited and is not used for commercial purposes.

DOI: 10.1002/adts.202200619

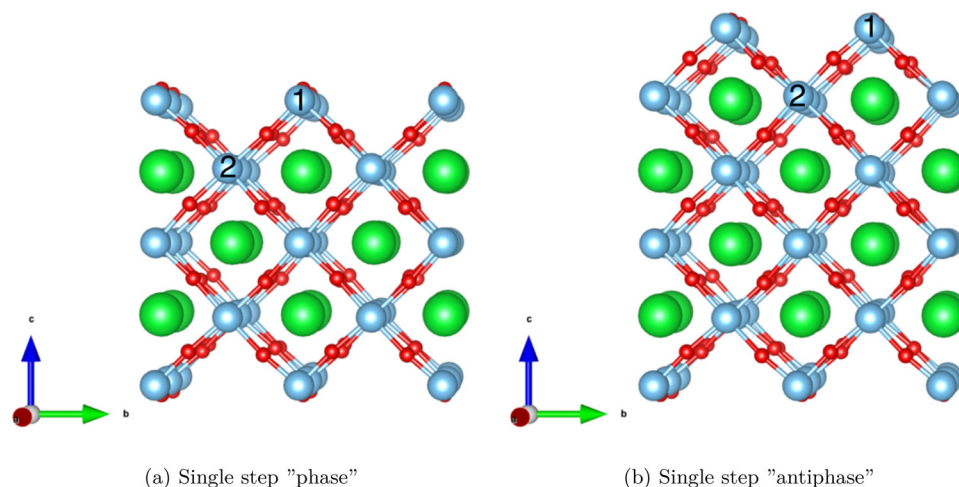


Figure 1. Flat surface cell. Green—Sr atoms, blue—Ti atoms, red—O atoms. Vacuum region is along the c vector. Reproduced under the terms and conditions of the Creative Commons Attribution CC BY license.^[19] Copyright 2021, The Authors, published by MDPI.

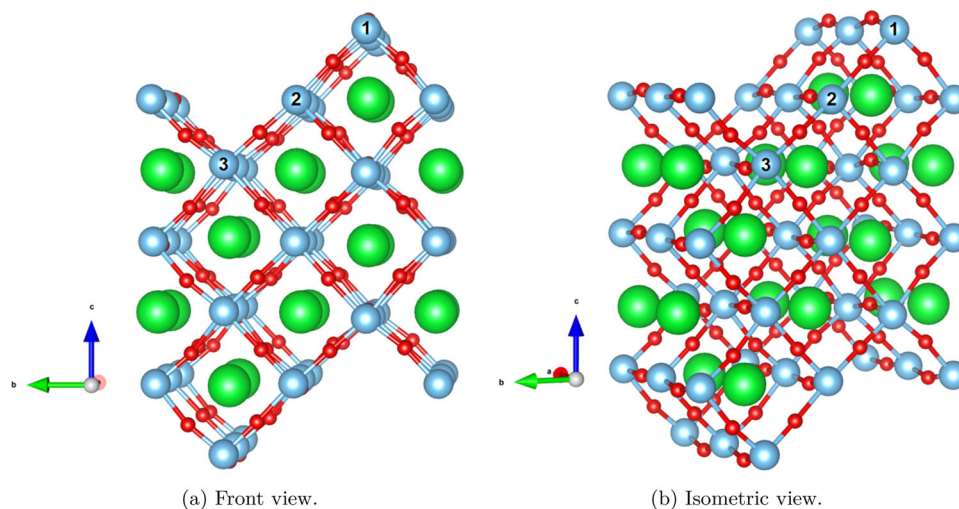


Figure 2. Single-stepped surface cell. 1—ridge adsorption site; 2—gully adsorption site. Green—Sr atoms, blue—Ti atoms, red—O atoms. Vacuum region is along the c vector.

mechanism can be observed for HER on stepped STO surfaces at low overpotentials. Investigation of V–H mechanism is out of scope of this paper.

Moreover, we apply computational hydrogen electrode (CHE) approach of Nørskov and Rossmeisel^[20,21] to estimate catalytic activity of both flat and stepped {110} surface toward HER. We use $\Delta\Delta G_{H^*}$ activity descriptor, which is similar to the approach described in ref. [22]. The reason to use $\Delta\Delta G_{H^*}$ over adsorption free energy ΔG_{H^*} is that the latter is very sensitive to exchange-correlation functional and inclusion or neglect of solvation effects. We demonstrate that flat surface is more active toward HER than stepped, even without considering charge recombination or presence of co-catalysts. This suggests that morphology of surfaces also plays a role in improved catalytic activity for HER, which, to the best of our knowledge, was not considered a factor in experimental studies of STO faceted nanoparticles.

2. Computational Details

Gas-phase density functional theory (DFT) calculations were performed with Vienna ab initio simulation package (VASP).^[23–26] Table S1, Supporting Information contains all necessary computational details. Relaxed rhombohedral SrTiO₃ phase ($R\bar{3}c$) with optimized lattice constant a_0 of 5.54 Å was used. We compare flat TiO₂-terminated {001} surface, single-lattice-constant $\frac{a_0}{\sqrt{2}}$ step {110} (single-stepped) and double-lattice-constant $\frac{a_0}{\sqrt{2}}$ step {110} (double-stepped) surface, shown in **Figures 1, 2, and 3**, respectively. Water molecules were placed on both terminations of the slab to neutralize electric dipole moment.

Water molecule adsorption energy ΔE_{ads} is calculated by Equation (4), where $E_{\text{H}_2\text{O}^*}$ is the total energy of configuration with water molecule adsorbed, E_* is the total energy of the corresponding surface without adsorbate and $E_{\text{H}_2\text{O}}$ is the total energy of water

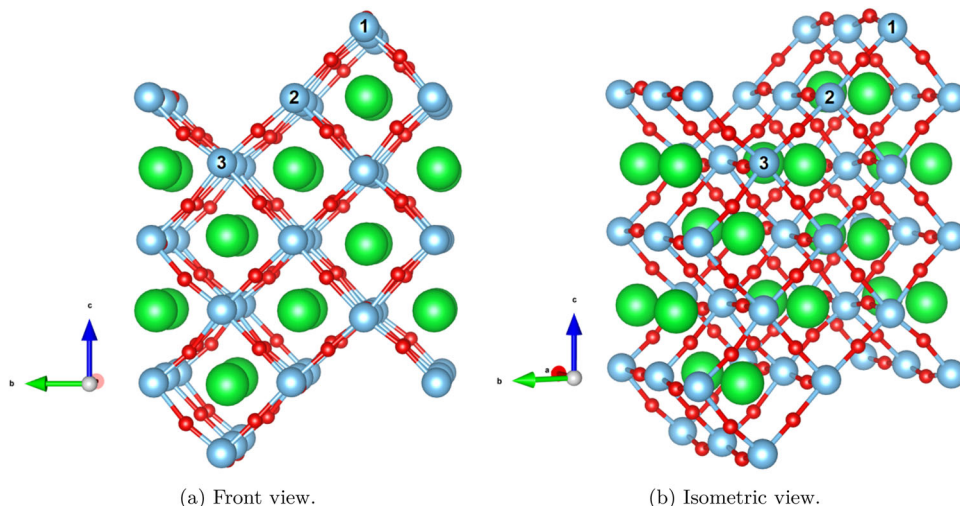


Figure 3. Double-stepped surface cell. 1—ridge adsorption site; 2—slope adsorption site; 3—gully adsorption site. Green—Sr atoms, blue—Ti atoms, red—O atoms. Vacuum region is along the c vector. Reproduced under the terms and conditions of the Creative Commons Attribution CC BY license.^[19] Copyright 2021, The Authors, published by MDPI.

molecule. The equation is written for non-symmetric slab, that is, single-sided adsorption.

$$\Delta E_{\text{ads}} = E_{\text{H}_2\text{O}^*} - (E_* + E_{\text{H}_2\text{O}}) \quad (4)$$

Water molecule adsorption free energy ΔG_{ads} is given by Equation (5) (for non-symmetric slab), where ZPE stands for zero-point energy, $\Delta \text{ZPE} = \text{ZPE}_{\text{H}_2\text{O}^*} - \text{ZPE}_{\text{H}_2\text{O}} - \text{ZPE}_*$ and $T\Delta S \approx -TS_{\text{H}_2\text{O}^*} - \text{ZPE}_{\text{H}_2\text{O}^*}$ (for each adsorption site) are calculated via finite differences method as implemented in VASP. $\text{ZPE}_{\text{H}_2\text{O}} = 0.57\text{eV}$ and $TS_{\text{H}_2\text{O}} = 0.67\text{eV}$ (at 298.15K and 0.035bar).^[20] By including the calculated values, we obtain $\Delta G_{\text{ads}} = \Delta E_{\text{ads}} + 0.53\text{eV}$ for ridge and $\Delta G_{\text{ads}} = \Delta E_{\text{ads}} + 0.79\text{eV}$ for slope.

$$\Delta G_{\text{ads}} = \Delta E_{\text{ads}} + \Delta \text{ZPE} - T\Delta S \quad (5)$$

We investigated the impact of water concentrations on the adsorption energies, and the impact is to a vast extend negligible, as described in Section S2, Supporting Information.

To perform thermodynamic simulations of HER, we calculate Gibbs free energy ΔG_{H^*} of Volmer step ($\text{H}^+ + \text{e}^- \rightarrow \text{H}^*$) by applying the CHE approach and using Equation (6)

$$\Delta G_{\text{H}^*} = E_{\text{H}^*} - E_* - \frac{1}{2}E_{\text{H}_2} + \Delta \text{ZPE} - T\Delta S \quad (6)$$

where H^* is hydrogen adsorbed on STO surface. $\Delta \text{ZPE} = \text{ZPE}_{\text{H}^*} - \frac{1}{2}\text{ZPE}_{\text{H}_2}$ with $\text{ZPE}_{\text{H}_2} = 0.27\text{eV}$ and $T\Delta S \approx -\frac{1}{2}TS_{\text{H}_2} = -0.20\text{eV}$.^[27] ZPE_{H^*} is calculated by using finite differences method as implemented in VASP. Please note that the Equation (6) is written for a non-symmetric slab (single-sided adsorption).

All figures are created in VESTA visualization system.^[28]

3. Results and Discussion

The section is structured as follows: first, we recap water adsorption on STO^[19] with additional insights on single-stepped surface. Second, we investigate water dissociation process on double-stepped surface. Finally, we discuss the results of CI-NEB calculations and thermodynamic simulations of HER.

3.1. Water Adsorption

To understand the difference between water adsorption on flat and stepped surface, we performed an extensive search of the most favorable water adsorption configuration and considered ≈ 50 initial geometries of a single water molecule per termination.^[19] In ref. [19] we discussed the most noteworthy ones.

The most important results of the previous study are that on flat surface dissociative adsorption is slightly more preferable and similar situation is observed on slope of the step. On ridge, only dissociative adsorption is possible, and it is accompanied by spontaneous oxygen vacancy formation. On gully, water adsorption is energetically less favorable.

Additionally, we performed calculations for a single-stepped surface. All energies are at HER conditions of $U = 0\text{V}$ versus RHE. Two variations of the single-stepped surface are considered: one where ridge of one side of the slab is directly opposite to ridge on the other side (“phase,” Figure 2a) and the other where ridge is directly opposite to gully (“antiphase,” Figure 2b). On the single-stepped surface (Figure 2) two modes of dissociative water adsorption are observed. Our results suggest that water adsorption configurations are the same on “phase” and “antiphase” single-stepped surface, so we visualize only “phase” in **Figure 4**. In ridge case, water molecule dissociates with spontaneous oxygen vacancy formation (“phase”: $\Delta G_{\text{ads}} = -1.04\text{eV}$; “antiphase”: $\Delta G_{\text{ads}} = -0.93\text{eV}$). The observed configuration and adsorption energy are almost identical to ridge of double-stepped surface.^[19]

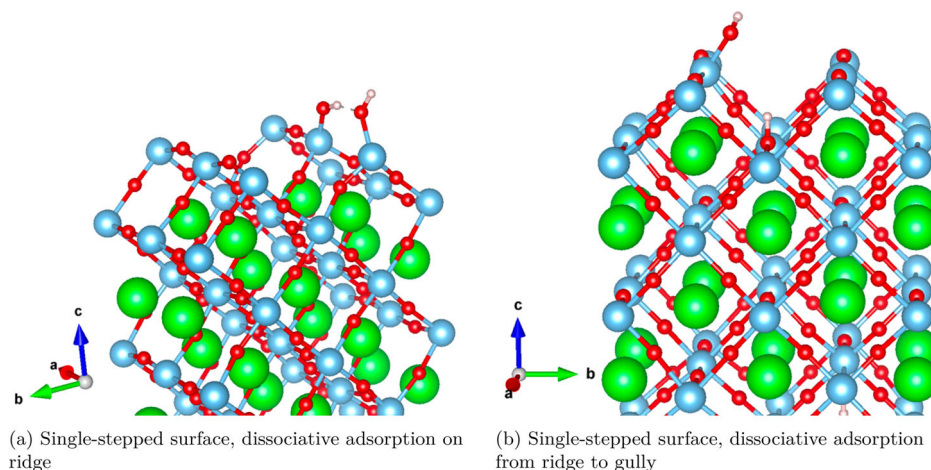


Figure 4. Water adsorption on single-stepped surface. Green—Sr atoms, blue—Ti atoms, red—O atoms, white—H atoms.

Another case is a less energetically favorable one with OH adsorbate atop ridge and the remaining H is atop gully (“phase”: $\Delta G_{\text{ads}} = -0.17$ eV; “antiphase”: $\Delta G_{\text{ads}} = -0.14$ eV). The slight difference in energetics can be explained by the shorter distance between adsorbates in “phase” surface.

3.2. Water Molecule Rotation and Proton Migration on the Double-Stepped Surface

To get insight into kinetic processes on the stepped surface we performed climbing image nudged elastic band (CI-NEB) calculations.^[29] Only processes around slope of the stepped surface were investigated, because only one very stable configuration was found for ridge and no noteworthy processes were found on gully. CI-NEB data are compiled in **Figure 5** for water rotation barriers and **Figure 6** for water dissociation barriers and for further proton migration. Detailed CI-NEB plots are in Supporting Information.

First, we investigated rotation of molecular water adsorbed on slope. We found that the rotation happens almost without energy barrier. The barrier of water molecule rotation from one orientation to another is below 0.10 eV (Figure 5).

Then we looked into water dissociation (Figure 6 reaction coordinate from 0 to 1 and Figures S2–S5, Supporting Information). Proton dissociates from water preferably along the slope with zero energy barrier, to a dissociative configuration that is slightly more stable than the molecular one. Dissociation toward gully is accompanied by at least 0.15 eV energy barrier, which is negligible at room temperature. Dissociation of the second proton is accompanied by a much higher barrier from 0.52 eV up to 0.60 eV, depending on initial configuration. Taking all of this into account means that water is predominantly adsorbed dissociatively along the slope and energy barriers make other configurations less likely. Dissociation barrier for flat surface is 0.09 eV, as reported in ref. [16], which is similar to the lowest dissociation barrier from our calculations for stepped surface.

After dissociation, the proton can migrate further. Preferable migration path is toward gully (Figure 6 and Figure S6, Support-

ing Information) with barrier 0.36 eV. Migration toward ridge (Figure 6 and Figure S7, Supporting Information) is less preferable with barrier 0.53 eV, which is consistent with observations from the geometry relaxation of the single-stepped surface. These barriers are also similar to the migration barrier on the flat surface, which is 0.51 eV.^[16]

Please note that some of the transition energy barriers are likely imprecise, since the performed frequency analysis of the supposed transition states revealed that the calculated minimum energy path goes through the stable intermediate instead of the expected saddle point. Pathways that go through the saddle point are drawn in bold in Figure 6.

3.3. Proton Migration Calculations in Context of HER Mechanism

Let us now discuss the possibility of V–T mechanism of HER on the STO stepped surface.

V–T mechanism requires two adjacent H* adsorbates. Thus, a sufficiently large H* coverage is expected. Also, the V–T mechanism comprises a chemical step (Tafel step), and this step is not affected by the applied electrode potential. Therefore, the free-energy barrier for the Tafel step needs to be sufficiently small so that the V–T mechanism can proceed.

V–H mechanism, on the other hand requires only a single H* adsorbate. Therefore, one may expect that the V–H mechanism may be operative even for a small H* coverage. Given that the V–H mechanism consists of electrochemical steps only that are affected by the applied electrode potential, one could expect that for sufficiently large overpotentials, the V–H mechanism generally excels the V–T mechanism.

We demonstrated the low energy barrier for H* migration so that two adjacent H* adsorbates are likely met, so the criteria of sufficiently large coverage is fulfilled. Hence, it is suggested that the V–T mechanism is possible for HER over STO stepped surface at low overpotentials. Yet, there is still an opportunity that the V–H mechanism is operative, and we cannot render a conclusion on which mechanism is energetically preferred, since the calculation of the transition states for the V–H mechanism is beyond the scope of the current paper.

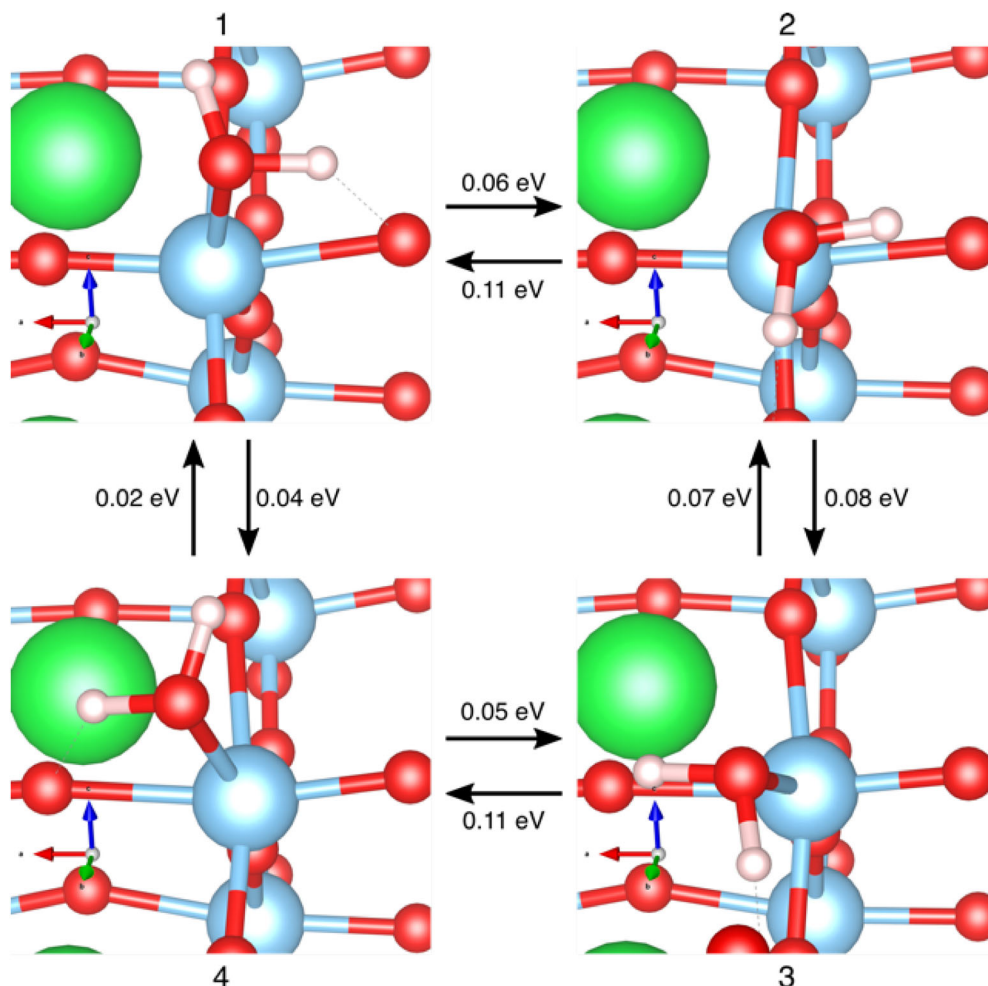


Figure 5. Molecular water rotation on slope of stepped surface. Arrows denote transition direction and numbers indicate height of transition barrier. $U = 0$ V versus RHE.

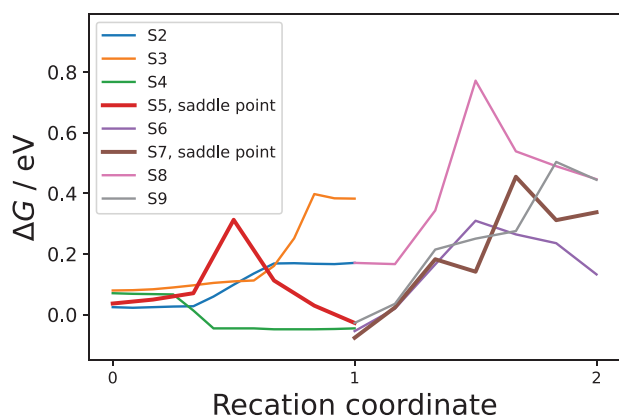


Figure 6. Free-energy diagram of water dissociation (reaction coordinate from 0 to 1) and further proton migration or *OH adsorbate dissociation (reaction coordinate from 1 to 2) in the vicinity of the slope of the double-stepped surface. $U = 0$ V versus RHE. Legend labels correspond to the number of the respective Figure in Supporting Information, where initial and final configurations are also shown.

3.4. HER

To estimate the catalytic activity of both flat and stepped surface we used a standard technique of computational hydrogen electrode approach.^[20,21] We placed a single hydrogen atom atop different oxygen sites, denoted similarly to Ti sites in Figure 3, with addition of ridge-slope and slope-gully sites, where H is placed atop O that is between the respective sites. Adsorption atop Ti was not considered, as calculation on flat surface revealed that Ti site to be vastly energetically unfavorable ($\Delta E_{\text{ads}} = 2.13$ eV).

As is known from experimental data on nanoparticles,^[15] HER occurs on the flat part of the nanoparticle, where Pt is deposited as co-catalyst. Thus we begin with comparing our ΔG_{H}^* value of flat STO surface (-0.13 eV) to that of platinum (-0.09 eV^[21]), which is by far the best catalyst for HER.^[30] As the values are close to each other, it can be concluded that flat STO surface is active toward HER, according to our calculations. This statement is valid independent of the fact that solvation, overpotential and kinetic effects may shift the optimum binding energy of adsorbed hydrogen away from zero,^[31–36] as gas-phase calculations are used

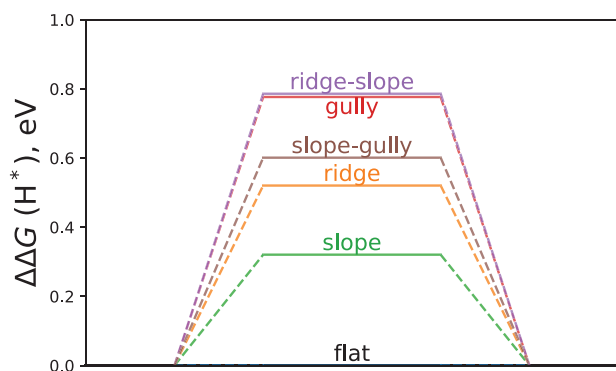


Figure 7. $\Delta\Delta G_{H^*}$ values with respect to flat STO surface.

Table 1. Data for Gibbs free energy calculation.

Site	$(E_{H^*} - E_s - E_{H_2})$ [eV]	ZPE _{H*} [eV]	ΔG_{H^*} [eV]
Flat	-0.51	0.32	-0.13
Ridge	0.00	0.32	0.39
Slope	-0.20	0.32	0.19
Gully	0.26	0.32	0.65
Ridge-slope	0.27	0.32	0.65
Slope-gully	0.09	0.31	0.47

here to capture general trends to distinguish between active or inactive sites.

To estimate the catalytic activity of other adsorption sites, we introduce $\Delta\Delta G_{H^*}$, defined in Equation (7). Similar approach is described in ref. [22]. In our study, $\Delta\Delta G_{H^*}$ is essentially ΔG_{H^*} of a system with respect to ΔG_{H^*} of the flat surface. The result is shown in **Figure 7** and data summarized in **Table 1**. We estimate error of our DFT calculations to be ≈ 0.1 eV, which is standard. This results in 0.2 eV error for $\Delta\Delta G_{H^*}$, except ΔG_{H^*} (flat), for which the error is 0.0 eV. Ridge, which is the second most active site, has $\Delta\Delta G_{H^*} = 0.32 \pm 0.2$ eV, and all other sites have $\Delta\Delta G_{H^*} > 0.32$ eV. Hence it can be concluded that the catalytic activity of STO nanoparticles toward HER is traced to the flat surface, when referring to the concept of ΔG_{H^*} as activity descriptor.

$$\Delta\Delta G_{H^*} = \Delta G_{H^*}(\text{system}) - \Delta G_{H^*}(\text{flat}) \quad (7)$$

4. Conclusions

In this work we presented results of our computational study of water dissociation, proton migration process, and HER on flat and stepped surface of STO.

CI-NEB calculations suggest that molecular water rotates freely atop slope. It then can dissociate along step virtually without barrier. The dissociated proton can further migrate toward ridge oxygen or gully oxygen, with the latter having lower barrier. The barriers of proton migration suggest that V-T mechanism of HER in case of incomplete coverage and low overpotentials is possible on slope of the step. Moreover, the barriers on slope of the step are similar to that of flat surface.

Thermodynamic simulations of HER concluded that flat surface is more catalytically active than stepped surface, which

means that not only charge separation and preferential co-catalyst deposition, but surface morphology itself plays a role in enhanced catalytic activity toward HER. The finding of better catalytic activity of the flat surface is consistent with the experimental data.

Supporting Information

Supporting Information is available from the Wiley Online Library or from the author.

Acknowledgements

The financial support of FLAG-ERA JTC project To2Dox is acknowledged by Y.M., G.Z., and E.K. This paper is based upon the work from COST Action 18234, supported by COST (European Cooperation in Science and Technology). The support is greatly acknowledged by Y.M., V.K., and K.S.E. The grant No. 1.1.1.2/VIAA/l/16/147 (1.1.1.2/16/l/001) under the activity of Post-doctoral research aid is greatly acknowledged by M.S. and D.B. K.S.E. acknowledges funding by the Ministry of Culture and Science of the Federal State of North Rhine-Westphalia (NRW Return Grant). K.S.E. is associated with the CRC/TRR247: "Heterogeneous Oxidation Catalysis in the Liquid Phase" (Project number 388390466-TRR 247), the RESOLV Cluster of Excellence, funded by the Deutsche Forschungsgemeinschaft under Germany's Excellence Strategy – EXC 2033 – 390677874 – RESOLV, and the Center for Nanointegration (CENIDE). Authors thank Dr. Marjeta Maček Kržmanc and Prof. Chi-Sheng Wu, for the fruitful discussions. The Institute of Solid State Physics, University of Latvia (Latvia) as the Centre of Excellence has received funding from the European Union's Horizon 2020 Framework Programme H2020-WIDESPREAD-01-2016-2017-Teaming Phase2 under grant agreement No. 739508, project CAMART². The computer resources were provided by the Stuttgart Supercomputing Center (project DEFTD 12939) and Latvian Super Cluster (LASC).

Open access funding enabled and organized by Projekt DEAL.

Conflict of Interest

The authors declare no conflict of interest.

Data Availability Statement

The data that support the findings of this study are available from the corresponding author upon reasonable request.

Keywords

ab initio, density functional theory, hydrogen evolution reaction, proton migration, SrTiO₃, stepped surface

Received: August 26, 2022

Revised: November 23, 2022

Published online:

- [1] H. Kato, A. Kudo, *J. Phys. Chem. B* **2002**, *106*, 5029.
- [2] M. Miyauchi, A. Nakajima, T. Watanabe, K. Hashimoto, *Chem. Mater.* **2002**, *14*, 2812.
- [3] R. Konta, T. Ishii, H. Kato, A. Kudo, *J. Phys. Chem. B* **2004**, *108*, 8992.
- [4] S. C. Yu, C. W. Huang, C. H. Liao, J. C. Wu, S. T. Chang, K. H. Chen, *J. Membr. Sci.* **2011**, *382*, 291.

- [5] H. Kato, M. Kobayashi, M. Hara, M. Kakihana, *Catal. Sci. Technol.* **2013**, *3*, 1733.
- [6] B. Wang, S. Shen, L. Guo, *Appl. Catal. B* **2015**, *166–167*, 320.
- [7] Y. Ham, T. Hisatomi, Y. Goto, Y. Moriya, Y. Sakata, A. Yamakata, J. Kubota, K. Domen, *J. Mater. Chem. A* **2016**, *4*, 3027.
- [8] P. Zhang, T. Ochi, M. Fujitsuka, Y. Kobori, T. Majima, T. Tachikawa, *Angew. Chem., Int. Ed.* **2017**, *56*, 5299.
- [9] G. S. Foo, Z. D. Hood, Z. Wu, *ACS Catal.* **2018**, *8*, 555.
- [10] D. Li, J. C.-C. Yu, V.-H. Nguyen, J. C. Wu, X. Wang, *Appl. Catal. B* **2018**, *239*, 268.
- [11] S. Kampouri, K. C. Stylianou, *ACS Catal.* **2019**, *9*, 4247.
- [12] T. Kanazawa, S. Nozawa, D. Lu, K. Maeda, *Catalysts* **2019**, *9*, 59.
- [13] Z. Saleem, E. Pervaiz, M. U. Yousaf, M. B. K. Niazi, *Catalysts* **2020**, *10*, 4.
- [14] M. Maček Kržmanc, N. Daneu, A. Čontala, S. Santra, K. M. Kamal, B. Likozar, M. Spreitzer, *ACS Appl. Mater. Interfaces* **2021**, *13*, 370.
- [15] L. Mu, Y. Zhao, A. Li, S. Wang, Z. Wang, J. Yang, Y. Wang, T. Liu, R. Chen, J. Zhu, F. Fan, R. Li, C. Li, *Energy Environ. Sci* **2016**, *9*, 2463.
- [16] H. Guhl, W. Miller, K. Reuter, *Phys. Rev. B: Condens. Matter Mater. Phys.* **2010**, *81*, 155455.
- [17] E. Holmström, P. Spijker, A. S. Foster, *Proc. R. Soc. A: Math. Phys. Eng. Sci* **2016**, *472*, 2193.
- [18] M. Cui, T. Liu, Q. Li, J. Yang, Y. Jia, *ACS Sustainable Chem. Eng.* **2019**, *7*, 15346.
- [19] M. Sokolov, Y. A. Mastrikov, G. Zvejnieks, D. Bocharov, E. A. Kotomin, V. Krasnenko, *Catalysts* **2021**, *11*, 1326.
- [20] J. K. Nørskov, J. Rossmeisl, A. Logadottir, L. Lindqvist, J. R. Kitchin, T. Bligaard, H. Jónsson, *J. Phys. Chem. B* **2004**, *108*, 17886.
- [21] J. K. Nørskov, T. Bligaard, A. Logadottir, J. R. Kitchin, J. G. Chen, S. Pandelov, U. Stimming, *J. Electrochem. Soc.* **2005**, *152*, J23.
- [22] T. Yang, J. Zhou, T. T. Song, L. Shen, Y. P. Feng, M. Yang, *ACS Energy Lett.* **2020**, *5*, 2313.
- [23] G. Kresse, J. Hafner, *Phys. Rev. B* **1993**, *47*, 558.
- [24] G. Kresse, J. Hafner, *Phys. Rev. B* **1994**, *49*, 14251.
- [25] G. Kresse, J. Furthmüller, *Comput. Mater. Sci.* **1996**, *6*, 15.
- [26] G. Kresse, J. Furthmüller, *Phys. Rev. B* **1996**, *54*, 11169.
- [27] Z. Liang, X. Zhong, T. Li, M. Chen, G. Feng, *ChemElectroChem* **2019**, *6*, 260.
- [28] K. Momma, F. Izumi, *J. Appl. Crystallogr.* **2011**, *44*, 1272.
- [29] D. Sheppard, P. Xiao, W. Chemelewski, D. D. Johnson, G. Henkelman, *J. Chem. Phys.* **2012**, *136*, 074103.
- [30] J. N. Hansen, H. Prats, K. K. Toudahl, N. Mørch Secher, K. Chan, J. Kibsgaard, I. Chorkendorff, *ACS Energy Lett.* **2021**, *6*, 1175.
- [31] H. Ooka, R. Nakamura, *J. Phys. Chem. Lett.* **2019**, *10*, 6706.
- [32] P. Lindgren, G. Kastlunger, A. A. Peterson, *ACS Catal.* **2020**, *10*, 121.
- [33] R. Kronberg, K. Laasonen, *ACS Catal.* **2021**, *11*, 8062.
- [34] H. Ooka, M. E. Wintzer, R. Nakamura, *ACS Catal.* **2021**, *11*, 6298.
- [35] K. S. Exner, *Int. J. Hydrog. Energy* **2020**, *45*, 27221.
- [36] K. S. Exner, *Curr. Opin. Electrochem.* **2021**, *26*, 100673.